Bioorganic & Medicinal Chemistry Letters 24 (2014) 667–673

Contents lists available at ScienceDirect

Bioorganic & Medicinal Chemistry Letters

journal homepage: www.elsevier.com/locate/bmcl

3D-QSAR study of adamantyl *N*-benzylbenzamides as melanogenesis inhibitors

Yong Deog Hong [a,*], Heung Soo Baek [a], Haelim Cho [b], Soo Mi Ahn [c], Ho Sik Rho [a], Young-Ho Park [a], Yung Hyup Joo [a], Song Seok Shin [a]

[a] *Materials Science, Medical Beauty Research Division, AmorePacific Corporation R&D Center, 314-1 Bora-Dong, Kiheung-Gu, Yongin-si, Kyounggi-do 446-729, South Korea*
[b] *T&J Tech Inc., Kasan-Dong, Keumchun-Gu, Seoul 153-770, South Korea*
[c] *Kyung Hee University Skin Biotechnology Center, Suwon 443-759, South Korea*

ARTICLE INFO

Article history:
Received 2 September 2013
Revised 4 November 2013
Accepted 22 November 2013
Available online 7 December 2013

Keywords:
CoMFA
CoMSIA
3D-QSAR
Melanogenesis
N-Benzylbenzamide

ABSTRACT

Three-dimensional quantitative structure–activity relationship (3D-QSAR) modeling, comparative molecular field analysis (CoMFA), and comparative molecular similarity indices analysis (CoMSIA) of polyhydroxylated *N*-benzylbenzamide derivatives containing an adamantyl moiety were performed to understand the mechanism of action and structure–activity relationship of these compounds. Contour map analysis indicated that steric contributions of the adamantyl moiety and electrostatic contributions of the hydroxyl group at the 3-position are important in the activity. Activities of the training set and test sets predicted by CoMFA fit well with actual activities, demonstrating that CoMFA, along with the best calculated q^2 value, has the best predictive ability.

Melanin plays a beneficial role in protecting the skin from various external stimuli, such as ultraviolet light, free radicals, and oxidative stresses. Melanogenesis is the biochemical process of melanin formation and its distribution within the skin. This, combined with the amount of melanin formed, determines skin color. Through the actions of various harmful stimuli, over-production of melanin from melanocytes leads to hyperpigmentation.[1,2] Therefore, the control of melanin synthesis via attenuation or inhibition of melanogenesis has received attention as a target treatment.[3,4]

Among the known depigmenting agents, we were interested in kazinols and broussonins, which contain a 1,3-diphenylpropane skeleton. These agents, which have strong depigmenting activity, have been used to design noble 1,3-diaryl polyhydroxy derivatives.[5] In an earlier study, we investigated polyhydroxylated *N*-benzylbenzamide derivatives that contain an adamantyl moiety, a new series of depigmenting agents with anti-melanogenic and tyrosinase-inhibiting activities.[6] We found that the depigmenting activities of these analogues could be modulated by altering their physicochemical properties via introduction of lipophilic or hydrophilic functionalities, such as variation of hydroxyl substituents, addition of a lipophilic adamantyl group, and modification of chain length. We tried to find the optimized hydroxyl group position for melanogenesis inhibition; modified hydroxyl substituents such as 3,4-dihydroxy, 2,5-dihydroxy, and 4-hydroxy groups on B ring showed the same tendency as in the case of 2,4-dihydroxy substitution, but were less effective toward melanogenesis inhibition. Also, the chain length between parts A and B appeared to have a relatively weak influence on the activity.

As an extension of this study, here we have prepared additional benzamide derivatives with various substituents and chain lengths. On the basis of this training set, we have performed studies to model three-dimensional quantitative structure–activity relationships (3D-QSARs) by comparative molecular field analysis (CoMFA) and comparative similarity indices analysis (CoMSIA)—methods which may provide further insight into the mechanism of action and optimal structure–activity relationships (SARs) of these compounds.

An initial set of 48 molecules was used for the 3D-QSAR modeling studies.[7] Both the training and test sets were designed to contain wide structural diversity and activity ranges. An extended dissimilarity selection method was used for finding a diverse representative subset using the SYBYL OpSim method; the test set molecules were selected with a diverse structure and activity pIC_{50} range (4.2596 to 5.9586).[8] The training set comprised 39 molecules containing an adamantyl or non-adamantyl moiety. The test set, which comprised 9 molecules considering their structural diversity and activity ranges, was used to validate the

* Corresponding author.
E-mail addresses: hydhong@amorepacific.com, hydhong@hanmail.com (S.S. Shin).

0960-894X/$ - see front matter © 2013 Elsevier Ltd. All rights reserved.
http://dx.doi.org/10.1016/j.bmcl.2013.11.056

developed CoMFA/CoMSIA model (Table 2). Melanogenesis inhibition data were obtained from a murine melanoma cell line (B16). The IC_{50} values of the 39 molecules in the training set, which were distributed over a wide range from 0.5 to 100 μM with respect to melanogenesis-inhibiting activity, were converted to pIC_{50} values for the 3D-QSAR studies. The calculated pIC_{50} values ranged from 4.1249 to 6.1367.

Compound 9 was used as the template for alignment in these studies because it showed the lowest IC_{50} values for biological activity. To align template molecules, the minimum energy conformation of 9 was sought by simulated annealing (heating the molecule at 700 K for 1000 fs and then annealing it to 200 K for 1000 fs). Subsequently, each molecule was structurally aligned on the basis of this conformation.[9] Following alignment, the steric and electrostatic potential fields for CoMFA/CoMSIA were calculated with a grid spacing of 2.0 Å by default and an attenuation factor of 0.3 (Fig. 1).

A comparison of the CoMFA model and each of the CoMSIA models is given in Table 1. Among the latter models, CoMSIA_all, which used all descriptors including steric, electrostatic, hydrophobic, H-donor, and H-acceptor, provided the best q^2 value of 0.691. Among all models, the CoMFA model had the highest q^2 value of 0.708. On the basis of this finding, we assumed that CoMFA was the best model in this study. The predicted and residual values for the CoMFA/CoMSIA models are described in Table 1, and the predicted versus actual pIC_{50} values are shown in Figure 2.

In Figure 2, the activities of both the training and test sets predicted by CoMFA fit well with the actual activities (r^2 = 0.839, slope of 0.839 for the training set; r^2 = 0.817, slope of 0.808 for the test and training sets). The blue data points correspond to the training set and red shows the test set. As illustrated in Figure 2B, the CoMSIA models displayed values slightly lower than those of the CoMFA model, e.g., for actual activities (r^2 = 0.827, slope of 0.827 for the training set; r^2 = 0.808, slope 0.794 for the test and training sets). Therefore, these results indicate that the CoMFA model has reliable predictive ability among the 3-D QSAR models. Analysis of the CoMFA model was provided by the following results.

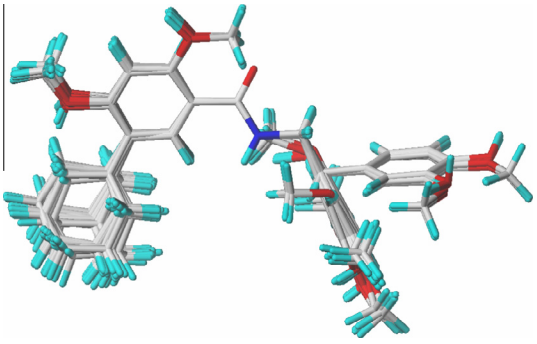

Figure 1. Alignment of molecules used in the training set.

From the data given in Table 1, the contributions of the steric and electrostatic fields of the CoMFA model are 56.6% and 43.4%, respectively. The steric fraction of molecules was also determined to play a slightly more significant role than the electrostatic fraction in predicting biological activity.

Table 3 provides a summary of the scrambling stability test results for the CoMFA model. The confidential Q^2 values should be high and near the 95% statistical confidence limit of 0.3,[10] and the calculated cross-validated standard error of prediction (cSDEP) should be low and similar to standard deviation of error of prediction (SDEP). In general, the effective slope ($dq^{2\prime}/dr^2_{yy'}$) is the most important value in the QSAR models.[11] Of these models, unstable ones are characterized by slopes greater than 1.20, whereas stable models have slopes near unity.[12] According to the summarized results, five components showed an acceptable range of slope values ($dq^{2\prime}/dr^2_{yy'}$). Of these five, component model 3 was optimal because it showed the highest Q^2 value of 0.597 and a $dq^{2\prime}/dr^2_{yy'}$ value nearest to unity. This was also in accordance with the partial least squares (PLS) results.

Contour maps of compound 9 in accord with these contributions are shown in Figure 3. Steric interactions are represented by the green and yellow contours, whereas electrostatic interactions are denoted by the red and blue contours. The steric contour maps (A) are shown in green when the activity increases with a large or bulky moiety. They are shown in yellow in the opposite case, that is, when the activity decreases.

Figure 3A depicts a sterically favored green contour located at the 3-position of 9, which suggests that biological activity increases with bulky adamantyl substitution. This trend is observed for all benzamide derivatives that possess an adamantyl substituent at the same position. Thus, compounds in the series, such as 15 with no substituent, exhibited reduced melanogenesis-inhibiting activities. The *para*-position (R^2) of 9 exhibited a sterically unfavored small yellow contour, suggesting that activity increases with the smaller OH group. However, more bulky substitution (methoxy) and smaller substituent H yielded reduced biological activity. Additionally, the B ring showed a yellow contour, and the small OH group increased melanogenesis-activity.

The electrostatic contour maps in Figure 3B are indicated in red when activity increases with negative atomic charges and in blue when activity increases with positive atomic charges. In general,

Table 1
Result of PLS (partial least square) analysis

Model	q^2	N	r^2	SEE	F	r^2_{pred}	Fraction				
							Steric	Electrostatic	Hydrophobic	H-donor	H-acceptor
CoMFA	0.708	3	0.839	0.193	60.608	0.739	0.566	0.434			
CoMSIA_all	0.691	3	0.827	0.200	55.805	0.737	0.181	0.258	0.257	0.182	0.122
CoMSIA_ES	0.683	3	0.814	0.207	51.156	0.711	0.370	0.630			
CoMSIA_ESH	0.690	3	0.818	0.205	52.487	0.710	0.223	0.451	0.325		
CoMSIA_DAH	0.692	4	0.851	0.188	48.734	0.744			0.513	0.294	0.192
CoMSIA_DA	0.038	5	0.550	0.332	8.062	−0.562				0.653	0.347

q^2: Leave-One-Out cross-validated correlation coefficient.
N: optimum number of components.
r^2: non-cross-validated correlation coefficient.
SEE: standard error of estimate.
F: *F*-test value.
r^2_{pred}: predictive r^2 for the test set.
Fraction: contribution rate of each CoMFA field.
S: steric, E: electrostatic, H: hydrophobic, D: H-donor, A: H-acceptor.

Table 2
Actual and CoMFA/CoMSIA-predicted pIC_{50} values of molecules in training and test sets

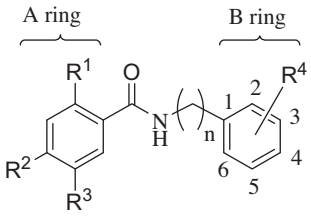

Compound	*n*	R^1	R^2	R^3	R^4	Actual pIC_{50}	CoMFA		CoMSIA_all	
							Pred. pIC_{50}	Residual	Pred. pIC_{50}	Residual
Training set										
3	1	OH	OH	H	2,4-OH	4.574	4.714	−0.141	4.761	−0.188
4	1	OH	OH	Ad[a]	2,4-OH	5.921	5.801	0.120	5.824	0.097
5	1	OH	OH	Ad	3,4-OH	5.602	5.809	−0.207	5.846	−0.244
6	2	OH	OH	Ad	3,4-OH	5.364	5.546	−0.183	5.553	−0.190
7	1	OH	OH	H	2,5-OH	4.616	4.694	−0.078	4.696	−0.080
8	1	OH	OH	Ad	2,5-OMe	5.387	5.441	−0.054	5.435	−0.048
9	1	OH	OH	Ad	2,5-OH	6.137	5.782	0.355	5.756	0.381
10	1	OMe	OMe	H	3,4-OH	5.046	5.020	0.026	5.019	0.027
11	1	H	OMe	H	3,4-OH	5.000	4.933	0.067	4.920	0.080
12	1	H	OMe	Ad	3,4-OH	5.652	5.922	−0.270	5.917	−0.265
13	1	OH	OMe	H	3,4-OH	5.097	4.979	0.118	4.972	0.125
14	2	OMe	OMe	Ad	4-OH	5.921	5.855	0.066	5.843	0.078
15	2	H	OH	H	3,4-OH	4.125	4.455	−0.330	4.465	−0.340
16	1	OMe	OMe	Ad	2,4-OH	5.959	5.956	0.003	6.013	−0.054
17	1	OH	OMe	Ad	3,4-OH	5.889	5.987	−0.098	5.976	−0.087
18	2	OH	OMe	Ad	3,4-OH	5.903	5.890	0.013	5.834	0.069
19	2	OH	OMe	Ad	4-OH	5.717	5.830	−0.113	5.788	−0.071
20	2	OMe	OMe	H	3,4-OH	4.959	4.759	0.200	4.742	0.217
21	1	OH	OMe	H	2,4-OH	4.559	4.930	−0.371	4.944	−0.385
22	1	H	OH	Ad	3,4-OH	5.590	5.737	−0.147	5.760	−0.170
23	2	H	OMe	Ad	3,4-OH	5.633	5.617	0.016	5.626	0.007
24	2	H	OMe	H	3,4-OH	4.638	4.666	−0.028	4.640	−0.002
25	1	H	OMe	Ad	2,4-OH	5.854	5.878	−0.024	5.881	−0.027
26	1	OH	OH	Ad	2-OMe	5.636	5.715	−0.079	5.539	0.097
27	1	OH	OH	Ad	4-OH	5.910	5.790	0.120	5.711	0.199
28	1	OH	OH	Ad	2,4-OMe	5.433	5.588	−0.155	5.505	−0.072
29	2	OH	OH	Ad	3,4-OMe	5.389	5.374	0.015	5.452	−0.063
30	1	OH	OH	Ad	3,4,5-OMe	5.532	5.323	0.209	5.361	0.171
31	1	OH	OH	Ad	3,4-OMe	5.419	5.392	0.027	5.367	0.052
32	2	H	OMe	Ad	3,4-OMe	5.347	5.485	−0.138	5.547	−0.200
33	1	H	OH	Ad	3,4-OMe	5.413	5.251	0.162	5.301	0.112
34	1	H	OH	Ad	2,5-OMe	5.267	5.343	−0.076	5.325	−0.058
35	1	H	OMe	Ad	3,4-OMe	5.301	5.413	−0.112	5.476	−0.175
36	1	H	OMe	Ad	3,5-OMe	5.299	5.465	−0.166	5.483	−0.184
37	1	H	OMe	Ad	2,5-OMe	5.503	5.516	−0.013	5.507	−0.004
38	2	H	OH	Ad	3,4-OH	5.680	5.449	0.231	5.482	0.198
39	1	OH	OH	Ad	3,5-OMe	5.590	5.399	0.191	5.427	0.163
40	2	OH	OMe	H	4-OH	5.301	4.811	0.490	4.780	0.521
41	1	H	OH	Ad	2,4-OH	6.046	5.695	0.351	5.733	0.313
Test set										
42	2	OH	OH	Ad	4-OH	5.959	5.666	0.293	5.662	0.297
43	1	OH	OMe	Ad	2,4-OH	5.745	5.925	−0.180	5.977	−0.232
44	1	OMe	OMe	H	2,4-OH	4.848	4.964	−0.116	5.004	−0.156
45	2	OMe	OMe	H	4-OH	4.569	4.860	−0.291	4.840	−0.271
46	1	H	OH	H	3,4-OH	4.260	4.693	−0.433	4.741	−0.481
47	2	H	OMe	Ad	4-OH	5.467	5.749	−0.282	5.714	−0.247
48	1	H	OH	Ad	3,5-OMe	5.353	5.303	0.050	5.305	0.048
49	1	OH	OH	H	3,4-OH	5.097	4.729	0.368	4.786	0.311
50	1	OH	OH	Ad	2-OH,4-OMe	5.243	5.544	−0.301	5.538	−0.295

[a] 1-Adamantyl.

red contour maps are assigned to heteroatoms such as nitrogen and oxygen, whose partial atomic charges are highly negative. The two large red contours indicated significant negative charges corresponding to OH groups located on the phenyl ring in 9, which are required for biological activity. The largely red contours located at the *para*-position (R^2) and 3-position of the B ring indicated that biological activity increases with the negative atomic charge of OH groups. Therefore, favorable steric and electrostatic contours provide an explanation for why compound 9 shows the best inhibitory activity among the series of adamantyl-substituted compounds.

CoMFA and CoMSIA studies were used to derive 3D-QSAR models for a training set of 39 benzamide derivatives. On the basis of the q^2 values, we chose CoMFA as the best validated 3D-QSAR model. Analysis of CoMFA studies yielded the following results:

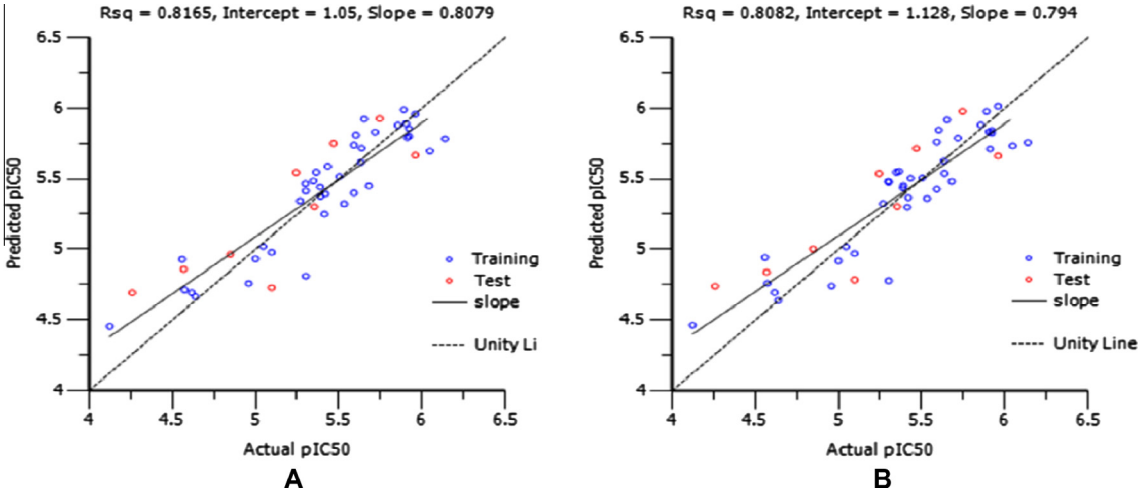

Figure 2. Plot of actual versus predicted activities for CoMFA (A) and CoMSIA (B).

Table 3
Result of scrambling stability test for CoMFA

#Component	Q^2	cSDEP	$dq^{2\prime}/dr^2_{yy'}$
1	0.486	0.335	0.535
2	0.585	0.304	0.731
3	0.597	0.304	0.973
4	0.543	0.326	0.695
5	0.497	0.351	0.715

Q^2; 1-$(cSDEP)^2$: predictive ability of the model after potential effects of redundancy have been removed; that is, the expected value of q^2 at the specified critical point. cSDEP: scaled cross-validated standard error, SDEP normalized by the standard deviation of the dependent variables.
$dq^{2\prime}/dr^2_{yy'}$: the slope of q^2 with respect to the correlation of the original dependent variables versus the perturbed dependent variables.

leave-one-out cross-validated q^2, 0.708; non cross-validated r^2, 0.839; F value, 60.608; standard error of estimation, 0.193; and predictive r^2 of test set, 0.739. The fractional contributions of the steric and electrostatic fields were 56.6% and 43.4%, respectively, in predicting biological activity. Additionally, the contour maps provided a viable explanation for the biological activities of our compounds. Accordingly, compound 42 in the test set, containing a 2,4-dihydroxy group on the B ring and lipophilic adamantyl group, showed the best correlation between actual biological activity and predictive activity. Therefore, our CoMFA results demonstrate an excellent correlation between steric/electrostatic fields and biological activity, and provide a deeper insight into the chemical structure design of new molecules with high melanogenesis-inhibiting activity. Among compounds 3, 6, 9, 16, 18, 27 and 41, which were shown to possess good anti-melanogenic activities, compound 16 (in-house library code: AP-736), which is also a good tyrosinase inhibitor, was selected as a promising candidate depigmenting agent with respect to large-scale preparation. Further evaluation of this compound is currently underway (Scheme 1).

Experimental section: *Chemistry:* ^{1}H NMR spectra were recorded on a Varian Mercury 300 spectrometer with DMSO-d_6 as solvent. Chemical shifts are reported in values (ppm) relative to the internal standard, and *J* values are reported in Hz. Mass spectra were recorded on an LCQ Deca XP plus LC/MS mass spectrometer. Reagents and solvents were purchased from common commercial suppliers and used without further purification.

Synthesis of substituted *N*-benzylbenzamide or *N*-phenethylbenzamide: *General procedures:* Substituted benzoic acid (2.1 mmol), *N*-hydroxysuccinimide (2.1 mmol), and *N*,*N*′-dicyclohexylcarbodiimide (2.1 mmol) were dissolved in 1,4-dioxane (5 mL) under a nitrogen atmosphere. The solution was stirred at ambient temperature for 12 h. The precipitate was filtered off and the filtrate added to a solution of substituted benzylamine HCl salt (2.3 mmol) and $NaHCO_3$ (2.3 mmol) in H_2O (2 mL). The reaction mixture was heated to 60 °C under nitrogen and stirred for 2–3 h. After cooling to room temperature, 10% HCl solution was added and the mixture was extracted with EtOAc. The combined organic layers were washed with brine, dried over anhydrous $MgSO_4$, and filtered, after which the filtrate was

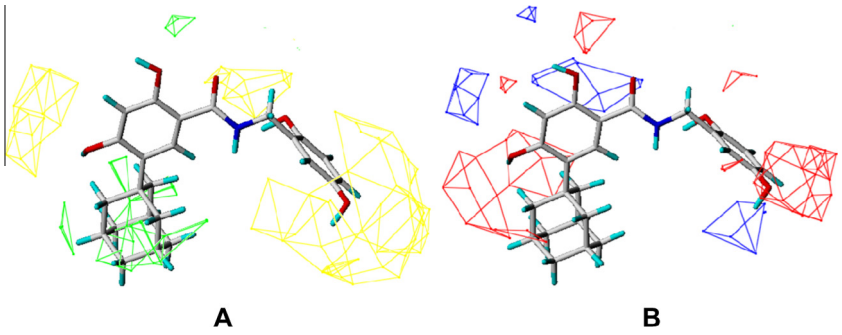

Figure 3. Contour maps of compound **10**. (A) Steric contour maps: green and yellow contours indicate regions where steric bulky groups increase and decrease activity, respectively. (B) Electrostatic contour maps: red and blue contours indicate regions where negative charge increases activity and positive charge increases activity, respectively.

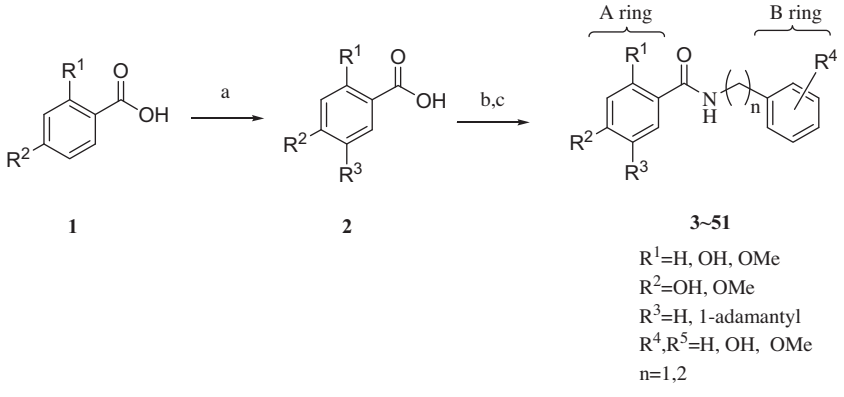

Scheme 1. General reagents and conditions: (a) 1-adamantanol, c-H_2SO_4/AcOH, CH_2Cl_2, rt; (b) HOSu, DCC, dioxane, rt; (c) Amine(salt), $NaHCO_3$, H_2O/50–60 °C, 3–4 h.

evaporated in vacuo. The crude product was purified by column chromatography to obtain the compound.

*N-(2,4-Dihydroxybenzyl)-2,4-dihydroxybenzamide (**3**):* ^{1}H NMR (300 MHz, DMSO-d_6): δ 12.71 (s, 1H), 10.00 (s, 1H), 9.39 (s, 1H), 9.08 (s, 1H), 8.75 (m, 1H), 7.73 (d, 1H, J = 8.4 Hz), 6.89 (d, 1H, J = 8.7 Hz), 6.24 (m, 3H), 6.15 (d, 1H, J = 8.7 Hz), 4.29 (d, 2H, J = 5.4 Hz); MS (EI): 275 (M^+).

*5-Adamantan-1-yl-N-(2,4-dihydroxybenzyl)-2,4-dihydroxybenzamide (**4**):* ^{1}H NMR (300 MHz, DMSO-d_6): δ 12.41 (s, 1H), 9.91 (s, 1H), 9.40 (s, 1H), 9.09 (s, 1H), 8.83 (m, 1H), 7.47 (s, 1H), 6.89 (d, 1H, J = 8.1 Hz), 6.26 (s, 2H), 6.16 (d, 1H, J = 8.1 Hz), 4.29 (m, 2H), 2.02 (s, 9H), 1.70 (s, 6H); MS (EI): 409 (M^+).

*5-Adamantan-1-yl-N-(3,4-dihydroxybenzyl)-2,4-dihydroxybenzamide (**5**):* ^{1}H NMR (300 MHz, DMSO-d_6): δ 12.74 (s, 1H), 9.95 (s, 1H), 8.98 (br s, 1H), 8.85 (s, 1H), 8.71 (s, 1H), 7.44 (s, 1H), 6.70 (s, 1H), 6.67–6.43 (m, 2H), 6.56–6.54 (m, 1H), 6.26 (s, 1H), 4.28 (d, 2H, J = 5.4 Hz), 2.03 (s, 9H), 1.71 (s, 6H); MS (EI): 409 (M^+).

*5-Adamantan-1-yl-N-[2-(3,4-dihydroxyphenyl)ethyl]-2,4-dihydroxybenzamide (**6**):* ^{1}H NMR (300 MHz, DMSO-d_6): δ 12.63 (s, 1H), 9.91 (s, 1H), 8.74 (s, 1H), 8.63 (s, 1H), 8.58 (br s, 1H), 7.38 (s, 1H), 6.65–6.61 (m, 2H), 6.48–6.45 (m, 1H), 6.25 (s, 1H), 3.45–3.40 (m, 2H), 2.65–2.60 (m, 2H), 2.03 (s, 9H), 1.72 (s, 6H); MS (EI): 423 (M^+).

*N-(2,5-Dihydroxybenzyl)-2,4-dihydroxybenzamide (**7**):* ^{1}H NMR (300 MHz, DMSO-d_6): δ 12.50 (s, 1H), 10.05 (s, 1H), 8.85 (br s, 1H), 8.80 (s, 1H), 8.60 (s, 1H), 7.80–7.75 (m, 1H), 6.65–6.25 (m, 5H), 4.38–4.30 (m, 2H); MS (EI): 275 (M^+).

*5-Adamantan-1-yl-N-(2,5-dimethoxybenzyl)-2,4-dihydroxybenzamide (**8**):* ^{1}H NMR (300 MHz, DMSO-d_6): δ 12.39 (s, 1H), 9.94 (s, 1H), 8.90 (br s, 1H), 7.50 (s, 1H), 6.93–6.72 (m, 3H), 6.28 (s, 1H), 4.40 (d, 2H, J = 5.7 Hz), 3.77 (s, 3H), 3.65 (s, 3H), 2.04 (s, 9H), 1.71 (s, 6H); MS (EI): 437 (M^+).

*5-Adamantan-1-yl-N-(2,5-dihydroxybenzyl)-2,4-dihydroxybenzamide (**9**):* ^{1}H NMR (300 MHz, DMSO-d_6): δ 12.50 (s, 1H), 9.94 (s, 1H), 8.92 (br s, 1H), 8.80 (s, 1H), 8.59 (s, 1H), 7.50 (s, 1H), 6.16–6.43 (m, 3H), 6.28 (s, 1H), 4.33 (d, 2H, J = 4.8 Hz), 2.04 (s, 9H), 1.71 (s, 6H); MS (EI): 409 (M^+).

*N-(3,4-Dihydroxybenzyl)-2,4-dimethoxybenzamide (**10**):* ^{1}H NMR (300 MHz, DMSO-d_6): δ 8.73 (br s, 1H), 8.34 (br s, 1H), 7.83 (d, 2H, J = 8.4 Hz), 6.70–6.54 (m, 5H), 4.31 (d, 2H, J = 5.7 Hz), 3.88 (s, 3H), 3.81 (s, 3H), 2.04 (s, 9H), 1.71 (s, 6H); MS (EI): 303 (M^+).

*N-(3,4-Dihydroxybenzyl)-4-methoxybenzamide (**11**):* ^{1}H NMR (300 MHz, DMSO-d_6): δ 8.72–8.59 (m, 3H), 7.77 (d, 2H, J = 8.4 Hz), 6.89 (d, 2H, J = 8.7 Hz), 6.61–6.44 (m, 3H), 4.19 (d, 2H, J = 5.7 Hz), 3.71 (s, 3H); MS (EI): 273 (M^+).

*3-Adamantan-1-yl-N-(3,4-dihydroxybenzyl)-4-methoxybenzamide (**12**):* ^{1}H NMR (300 MHz, DMSO-d_6): δ 8.74 (br s, 1H), 7.76–7.70 (m, 2H), 7.03–7.00 (m, 1H), 6.70–6.53 (m, 3H), 4.27 (d, 2H, J = 6.0 Hz), 3.84 (s, 3H), 2.05 (s, 9H), 1.73 (s, 6H); MS (EI): 407 (M^+).

*N-(3,4-Dihydroxybenzyl)-2-hydroxy-4-methoxybenzamide (**13**):* ^{1}H NMR (300 MHz, DMSO-d_6): δ 13.11 (s, 1H), 9.05 (br s, 1H), 8.86 (s, 1H), 8.74 (s, 1H), 7.83–7.80 (m, 2H), 6.70–6.41 (m, 5H), 4.30 (d, 2H, J = 5.7 Hz), 3.76 (s, 3H); MS (EI): 289 (M^+).

*5-Adamantan-1-yl-N-[2-(4-hydroxyphenyl)ethyl]-2,4-dimethoxybenzamide (**14**):* ^{1}H NMR (300 MHz, DMSO-d_6): δ 9.20 (s, 1H), 7.94 (br s, 1H), 7.73 (s, 1H), 7.04 (d, 2H, J = 8.1 Hz), 6.71 (d, 2H, J = 8.1 Hz), 6.63 (s, 1H), 3.87 (s, 3H), 3.84 (s, 3H), 3.45–3.43 (m, 2H), 2.71–2.66 (m, 2H), 1.99 (s, 9H), 1.71 (s, 6H); MS (EI): 435 (M^+).

*N-[2-(3,4-Dihydroxyphenyl)ethyl]-4-hydroxybenzamide (**15**):* ^{1}H NMR (300 MHz, DMSO-d_6): δ 9.89 (br s, 1H), 8.68 (br s, 1H), 8.22 (br s, 1H), 7.68 (d, 2H, J = 8.4 Hz), 6.77 (d, 2H, J = 8.4 Hz), 6.63–6.43 (m, 3H), 3.40–3.35 (m, 2H), 2.63–2.58 (m, 2H); MS (EI): 273 (M^+).

*5-Adamantan-1-yl-N-(2,4-dihydroxybenzyl)-2,4-dimethoxybenzamide (**16**):* ^{1}H NMR (300 MHz, DMSO-d_6): δ 9.67 (s, 1H), 9.13 (s, 1H), 8.51 (m, 1H), 7.78 (m, 1H), 6.92 (d, 1H, J = 8.1 Hz), 6.66 (s, 1H), 6.27 (s, 1H), 6.16 (d, 1H, J = 8.1 Hz), 4.30 (d, 2H, J = 5.4 Hz), 3.93 (s, 3H), 3.88 (s, 3H), 1.98 (s, 9H), 1.71 (s, 6H); MS (EI): 437 (M^+).

5-Adamantan-1-yl-*N*-(3,4-dihydroxybenzyl)-2-hydroxy-4-*methoxybenzamide (**17**):* ^{1}H NMR (300 MHz, DMSO-d_6): δ 12.99 (s, 1H), 9.09 (br s, 1H), 8.85 (s,1H), 8.72 (s, 1H), 7.48 (s, 1H), 6.71–6.43 (m, 4H), 4.30 (d, 2H, J = 5.4 Hz), 3.79 (s, 3H), 3.88 (s, 3H), 2.00 (s, 9H), 1.71 (s, 6H); MS (EI): 423 (M^+).

*5-Adamantan-1-yl-N-[2-(3,4-dihydroxyphenyl)-ethyl]-2-hydroxy-4-methoxybenzamide (**18**):* ^{1}H NMR (300 MHz, DMSO-d_6): δ 12.89 (s, 1H), 8.76–8.65 (m, 3H), 7.43 (s, 1H), 6.65–6.42 (m, 4H), 3.79 (s, 3H), 3.40–3.36 (m, 2H), 2.66–2.62 (m, 2H), 2.01 (s, 9H), 1.72 (s, 6H); MS (EI): 437 (M^+).

*5-Adamantan-1-yl-2-hydroxy-N-[2-(4-hydroxyphenyl)ethyl]-4-methoxybenzamide (**19**):* ^{1}H NMR (300 MHz, DMSO-d_6): δ 12.85 (s, 1H), 9.17 (s, 1H), 8.70 (br s, 1H), 7.42 (s, 1H), 7.02 (d, 2H, J = 8.1 Hz), 6.68 (d, 2H, J = 8.1 Hz), 6.41 (s, 1H), 3.78 (s, 3H), 3.50–3.39 (m, 2H), 2.73–2.71 (m, 2H), 2.00 (s, 9H), 1.72 (s, 6H); MS (EI): 421 (M^+).

*N-[2-(3,4-Dihydroxyphenyl)ethyl]-2,4-dimethoxybenzamide (**20**):* ^{1}H NMR (300 MHz, DMSO-d_6): δ 8.77 (br s, 1H), 8.67 (br s, 1H), 7.94 (br s, 1H), 7.84–7.81 (m, 2H), 6.67–6.47 (m, 5H), 3.81 (s, 3H), 3.80 (s, 3H), 3.50–3.41 (m, 2H), 2.64–2.60 (m, 2H); MS (EI): 317 (M^+).

*N-(2,4-Dihydroxybenzyl)-2-hydroxy-4-methoxybenzamide (**21**):* ^{1}H NMR (300 MHz, DMSO-d_6): δ 12.91 (s, 1H), 9.40 (s, 1H), 9.12 (s, 1H), 8.86 (m, 1H), 7.85 (d, 1H, J = 8.7 Hz), 6.90 (d, 1H, J = 8.7 Hz), 6.44 (m, 2H), 6.28 (s, 1H), 6.16 (d, 1H, J = 8.1 Hz), 4.31 (d, 2H, J = 5.1 Hz), 3.76 (s, 3H); MS (EI): 289 (M^+).

*3-Adamantan-1-yl-N-(3,4-dihydroxybenzyl)-4-hydroxybenzamide (**22**):* ^{1}H NMR (300 MHz, DMSO-d_6): δ 9.82 (br s, 1H), 8.80–8.60 (m, 3H), 7.63 (s, 1H), 7.56 (d, 1H, J = 8.1 Hz), 6.77 (d, 1H, J = 8.4 Hz),

6.69 (s, 1H), 6.64 (d, 1H, J = 8.1 Hz), 6.53 (d, 1H, J = 8.1 Hz), 4.26 (d, 2H, J = 6.0 Hz), 2.07 (s, 9H), 1.72 (s, 6H); MS (EI): 393 (M^+).

*3-Adamantan-1-yl-N-[2-(3,4-dihydroxyphenyl)ethyl]-4-methoxybenzamide (**23**):* ^{1}H NMR (300 MHz, DMSO-d_6): δ 8.73 (br s, 1H), 8.63 (br s, 1H), 8.34 (br s, 1H), 7.68–7.63 (m, 2H), 6.99 (d, 1H, J = 8.7 Hz), 6.64–6.60 (m, 2H), 6.46 (d, 1H, J = 8.1 Hz), 3.83 (s, 3H), 3.40–3.35 (m, 2H), 2.64–2.59 (m, 2H), 2.05 (s, 9H), 1.73 (s, 6H); MS (EI): 421 (M^+).

*N-[2-(3,4-Dihydroxyphenyl)ethyl]-4-methoxybenzamide (**24**):* ^{1}H NMR (300 MHz, DMSO-d_6): δ 8.71 (br s, 1H), 8.63 (br s, 1H), 8.34 (br s, 1H), 7.79 (d, 2H, J = 8.7 Hz), 6.97 (d, 2H, J = 8.7 Hz), 6.64–6.61 (m, 2H), 6.46 (d, 1H, J = 8.1 Hz), 3.80 (s, 3H), 3.45–3.35 (m, 2H), 2.65–2.60 (m, 2H); MS (EI): 287 (M^+).

*3-Adamantan-1-yl-N-(2,4-dihydroxybenzyl)-4-methoxybenzamide (**25**):* ^{1}H NMR (300 MHz, DMSO-d_6): δ 9.58 (s, 1H), 9.09 (s, 1H), 8.81 (t, 1H, J = 5.4 Hz), 7.73 (m, 2H), 7.02 (d, 1H, J = 8.4 Hz), 6.90 (d, 1H, J = 8.1 Hz), 6.18 (m, 2H), 4.26 (d, 2H, J = 5.7 Hz), 3.84 (s, 3H), 2.05 (s, 9H), 1.73 (s, 6H); MS (EI): 407 (M^+).

*5-Adamantan-1-yl-2,4-dihydroxy-N-(2-methoxybenzyl)benzamide (**26**):* ^{1}H NMR (300 MHz, DMSO-d_6): δ 12.46 (s, 1H), 9.93 (s, 1H), 8.93 (br s, 1H), 7.51 (s, 1H), 7.26–6.87 (m, 4H), 6.28 (s, 1H), 4.43 (d, 2H, J = 5.4 Hz), 3.82 (s, 3H), 2.04 (s, 9H), 1.71 (s, 6H); MS (EI): 407 (M^+).

*5-Adamantan-1-yl-2,4-dihydroxy-N-(4-hydroxybenzyl)benzamide (**27**):* ^{1}H NMR (300 MHz, DMSO-d_6): δ 12.68 (s, 1H), 9.94 (s, 1H), 9.26 (s, 1H), 8.98 (m, 1H), 7.42 (s, 1H), 7.11 (d, 2H, J = 8.1 Hz), 6.70 (d, 2H, J = 8.1 Hz), 6.24 (s, 1H), 4.33 (m, 2H), 2.02 (s, 9H), 1.70 (s, 6H); MS (EI): 393 (M^+).

*5-Adamantan-1-yl-N-(2,4-dimethoxybenzyl)-2,4-dihydroxybenzamide (**28**):* ^{1}H NMR (300 MHz, DMSO-d_6): δ 12.48 (s, 1H), 9.92 (s, 1H), 8.86 (m, 1H), 7.48 (s, 1H), 7.07 (d, 1H, J = 8.1 Hz), 6.56 (m, 1H), 6.48 (m, 1H), 6.27 (s, 1H), 6.18 (m, 2H),, 4.35 (d, 2H, J = 5.4 Hz), 3.80 (s, 3H), 3.73 (s, 3H), 2.03 (s, 9H), 1.71 (s, 6H); MS (EI): 437 (M^+).

*5-Adamantan-1-yl-N-[2-(3,4-dimethoxyphenyl)ethyl]-2,4-dihydroxybenzamide (**29**):* ^{1}H NMR (300 MHz, DMSO-d_6): δ 12.58 (s, 1H), 9.90 (s, 1H), 8.56 (br s, 1H), 7.37 (s, 1H), 6.87–6.75 (m, 3H), 6.24 (s, 1H), 3.70 (s, 6H), 3.50–3.35 (m, 2H), 2.78–2.76 (m, 2H), 2.02 (s, 9H), 1.72 (s, 6H); MS (EI): 451 (M^+).

*5-Adamantan-1-yl-2,4-dihydroxy-N-(3,4,5-trimethoxybenzyl)benzamide (**30**):* ^{1}H NMR (300 MHz, DMSO-d_6): δ 12.51 (s, 1H), 9.95 (s, 1H), 8.99 (br s, 1H), 7.46 (s, 1H), 6.67–6.64 (m, 2H), 6.27 (s, 1H), 4.39 (d, 2H, J = 5.4 Hz), 3.74 (s, 6H), 3.62 (s, 3H), 2.03 (s, 9H), 1.71 (s, 6H); MS (EI): 467 (M^+).

*5-Adamantan-1-yl-N-(3,4-dimethoxy-benzyl)-2,4-dihydroxy-benzamide (**31**):* ^{1}H NMR (300 MHz, DMSO-d_6): δ 12.62 (s, 1H), 9.96 (s, 1H), 9.01 (br s, 1H), 7.44 (s, 1H), 6.93–6.84 (m, 3H), 6.26 (s, 1H), 4.38 (d, 2H, J = 5.4 Hz), 3.73 (s, 3H), 3.71 (s, 3H), 2.03 (s, 9H), 1.71 (s, 6H); MS (EI): 437 (M^+).

*3-Adamantan-1-yl-N-[2-(3,4-dimethoxyphenyl)ethyl]-4-methoxybenzamide (**32**):* ^{1}H NMR (300 MHz, DMSO-d_6): δ 8.34 (s, 1H), 7.68–7.62 (m, 2H), 7.00 (d, 1H, J = 8.4 Hz), 6.86–6.72 (m, 3H), 3.83 (s, 3H), 3.70 (s, 6H), 3.50–3.35 (m, 2H), 2.77–2.73 (m, 2H), 2.04 (s, 9H), 1.73 (s, 6H); MS (EI): 449 (M^+).

*3-Adamantan-1-yl-N-(3,4-dimethoxybenzyl)-4-hydroxybenzamide (**33**):* ^{1}H NMR (300 MHz, DMSO-d_6): δ 9.83 (s, 1H), 8.67 (br s, 1H), 7.63–7.55 (m, 2H), 6.92–6.76 (m, 4H), 4.36 (d, 2H, J = 5.7 Hz), 3.72 (s, 3H), 3.71 (s, 3H), 2.07 (s, 9H), 1.72 (s, 6H); MS (EI): 421 (M^+).

*3-Adamantan-1-yl-N-(2,5-dimethoxybenzyl)-4-hydroxybenzamide (**34**):* ^{1}H NMR (300 MHz, DMSO-d_6): δ 9.85 (br s, 1H), 8.57 (br s, 1H), 7.65–7.57 (m, 2H), 6.90–6.71 (m, 4H), 4.37 (d, 2H, J = 5.7 Hz), 3.76 (s, 3H), 3.64 (s, 3H), 2.08 (s, 9H), 1.73 (s, 6H); MS (EI): 421 (M^+).

*3-Adamantan-1-yl-N-(3,4-dimethoxybenzyl)-4-methoxybenzamide (**35**):* ^{1}H NMR (300 MHz, DMSO-d_6): δ 8.79 (br s, 1H), 7.75–7.69 (m, 2H), 7.03–6.80 (m, 4H), 4.39 (d, 2H, J = 6.0 Hz), 3.84 (s, 3H), 3.72 (s, 3H), 3.71 (s, 3H), 2.05 (s, 9H), 1.73 (s, 6H); MS (EI): 435 (M^+).

*3-Adamantan-1-yl-N-(3,5-dimethoxybenzyl)-4-methoxybenzamide (**36**):* ^{1}H NMR (300 MHz, DMSO-d_6): δ 8.83 (br s, 1H), 7.77–7.70 (m, 2H), 7.03 (d, 1H, J = 8.4 Hz), 6.46 (s, 2H), 6.36 (s, 1H), 4.38 (d, 2H, J = 5.4 Hz), 3.84 (s, 3H), 3.70 (s, 6H), 2.05 (s, 9H), 1.73 (s, 6H); MS (EI): 435 (M^+).

*3-Adamantan-1-yl-N-(2,5-dimethoxybenzyl)-4-methoxybenzamide (**37**):* ^{1}H NMR (300 MHz, DMSO-d_6): δ 8.70 (br s, 1H), 7.78–7.71 (m, 2H), 7.03 (d, 1H, J = 8.7 Hz), 6.90 (d, 1H, J = 8.7 Hz), 6.79–6.72 (m, 2H), 4.39 (d, 2H, J = 6.0 Hz), 3.85 (s, 3H), 3.77 (s, 3H), 3.64 (s, 3H), 2.05 (s, 9H), 1.73 (s, 6H); MS (EI): 435 (M^+).

*3-Adamantan-1-yl-N-[2-(3,4-dihydroxyphenyl)ethyl]-4-hydroxybenzamide (**38**):* ^{1}H NMR (300 MHz, DMSO-d_6): δ 9.80 (br s, 1H), 8.70 (br s, 1H), 8.22 (br s, 1H), 7.57–7.48 (m, 2H), 6.77–6.43 (m, 4H), 3.45–3.35 (m, 2H), 2.62–2.58 (m, 2H), 2.07 (s, 9H), 1.73 (s, 6H); MS (EI): 407 (M^+).

*5-Adamantan-1-yl-N-(3,5-dimethoxybenzyl)-2,4-dihydroxybenzamide (**39**):* ^{1}H NMR (300 M Hz, DMSO-d_6): δ 12.6 (br s, 1H), 9.96 (s, 1H), 9.04 (br s, 1H), 7.46 (s, 1H), 6.46 (s, 2H), 6.38 (s, 1H), 6.27 (s, 1H), 4.39 (d, 2H, J = 5.4 Hz), 3.71 (s, 6H), 2.04 (s, 9H), 1.71 (s, 6H); MS (EI): 437 (M^+).

*2-Hydroxy-N-[2-(4-hydroxyphenyl)ethyl]-4-methoxybenzamide (**40**):* ^{1}H NMR (300 MHz, DMSO-d_6): δ 13.0 (br s, 1H), 9.17 (s, 1H), 8.68 (br s, 1H), 7.77 (d, 1H, J = 8.7 Hz), 7.02 (d, 2H, J = 7.5 Hz), 6.67 (d, 2H, J = 7.5 Hz), 6.46–6.40 (m, 2H), 3.76 (s, 3H), 3.45–3.38 (m, 2H), 2.74–2.69 (m, 2H); MS (EI): 287 (M^+).

*3-Adamantan-1-yl-N-(2,4-dihydroxybenzyl)-4-hydroxybenzamide (**41**):* ^{1}H NMR (300 MHz, DMSO-d_6): δ 9.87 (br s, 1H), 9.64 (s, 1H), 9.09 (s, 1H), 8.73 (br s, 1H), 7.63–7.55 (m, 2H), 6.89 (d, 1H, J = 8.1 Hz), 6.78 (d, 1H, J = 7.8 Hz), 6.23–6.15 (m, 2H), 4.25 (m, 2H), 2.07 (s, 9H), 1.72 (s, 6H); MS (EI): 393 (M^+).

*5-Adamantan-1-yl-2,4-dihydroxy-N-[2-(4-hydroxyphenyl)ethyl]benzamide (**42**):* ^{1}H NMR (300 MHz, DMSO-d_6): δ 12.59 (s, 1H), 9.91 (s, 1H), 9.16 (s, 1H), 8.60 (br s, 1H), 7.38 (s, 1H), 7.03–7.00 (m, 2H), 6.69–6.66 (m, 2H), 6.25 (s, 1H), 3.40–3.35 (m, 2H), 2.72–2.67 (m, 2H), 2.03 (s, 9H), 1.72 (s, 6H); MS (EI): 407 (M^+).

*5-Adamantan-1-yl-N-(2,4-dihydroxybenzyl)-2-hydroxy-4-methoxybenzamide (**43**):* ^{1}H NMR (300 MHz, DMSO-d_6): δ 12.73 (s, 1H), 9.40 (s, 1H), 9.11 (s, 1H), 8.95 (m, 1H), 7.52 (s, 1H), 6.90 (d, 1H, J = 8.4 Hz), 6.43 (s, 1H), 6.28 (s, 1H), 6.17 (d, 1H, J = 8.4 Hz), 4.31 (d, 2H, J = 5.4 Hz), 3.79 (s, 3H), 2.00 (s, 9H), 1.71 (s, 6H); MS (EI): 423 (M^+).

*N-(2,4-Dihydroxybenzyl)-2,4-dimethoxybenzamide (**44**):* ^{1}H NMR (300 MHz, DMSO-d_6): δ 9.65 (s, 1H), 9.13 (s, 1H), 8.52 (m, 1H), 7.87 (d, 1H, J = 8.4 Hz), 6.93 (d, 1H, J = 8.7 Hz), 6.63 (m, 2H), 6.28 (s, 1H), 6.16 (d, 1H, J = 8.1 Hz), 4.30 (d, 2H, J = 5.7 Hz), 3.90 (s, 3H), 3.81 (s, 3H); MS (EI): 303 (M^+).

*N-[2-(4-Hydroxyphenyl)ethyl]-2,4-dimethoxybenzamide (**45**):* ^{1}H NMR (300 MHz, DMSO-d_6): δ 9.19 (s, 1H), 7.95 (br s, 1H), 7.82 (d, 1H, J = 9.3 Hz), 7.04 (d, 2H, J = 7.5 Hz), 6.70 (d, 2H, J = 7.5 Hz), 6.62 (m, 2H), 3.81 (s, 3H), 3.80 (s, 3H), 3.48–3.41 (m, 2H), 2.72–2.67 (m, 2H); MS (EI): 301 (M^+).

*N-(3,4-Dihydroxybenzyl)-4-hydroxybenzamide (**46**):* ^{1}H NMR (300 MHz, DMSO-d_6): δ 9.92 (br s, 1H), 8.79 (br s, 1H), 8.66–8.61 (m, 2H), 7.75 (d, 2H, J = 8.7 Hz), 6.78 (d, 2H, J = 8.4 Hz), 6.69 (s, 1H), 6.64 (d, 1H, J = 7.8 Hz), 6.54 (d, 1H, J = 7.8 Hz), 4.26 (d, 2H, J = 8.4 Hz); MS (EI): 259 (M^+).

*3-Adamantan-1-yl-N-[2-(4-hydroxyphenyl)ethyl]-4-methoxybenzamide (**47**):* ^{1}H NMR (300 MHz, DMSO-d_6): δ 9.14 (s, 1H), 8.33 (br s, 1H), 7.67–7.63 (m, 2H), 7.02–6.98 (m, 3H), 6.67 (d, 2H, J = 8.1 Hz), 3.83 (s, 3H), 3.40–3.35 (m, 2H), 2.72–2.67 (m, 2H), 2.05 (s, 9H), 1.74 (s, 6H); MS (EI): 405 (M^+).

*3-Adamantan-1-yl-N-(3,5-dimethoxybenzyl)-4-hydroxybenzamide (**48**):* ^{1}H NMR (300 MHz, DMSO-d_6): δ 9.85 (s, 1H), 8.71 (br s, 1H), 7.64–7.56 (m, 2H), 6.78 (d, 1H, J = 7.8 Hz), 6.45 (s, 2H), 6.36 (s,

1H), 4.36 (d, 2H, J = 5.4 Hz), 3.71 (s, 6H), 2.08 (s, 9H), 1.73 (s, 6H); MS (EI): 421 (M^+).

*N-(3,4-Dihydroxybenzyl)-2,4-dihydroxybenzamide (**49**):* ^{1}H NMR (300 MHz, DMSO-d_6): δ 12.5 (br s, 1H), 10.07 (br s, 1H), 8.90–8.72 (m, 3H), 7.70 (d, 1H, J = 8.7 Hz), 6.69–6.21 (m, 5H), 4.28 (d, 2H, J = 5.4 Hz); MS (EI): 275 (M^+).

*5-Adamantan-1-yl-2,4-dihydroxy-N-(2-hydroxy-4-methoxybenzyl)benzamide (**50**):* ^{1}H NMR (300 MHz, DMSO-d_6): δ 12.39 (br s, 1H), 9.92 (s, 1H), 9.65 (s, 1H), 8.89 (br s, 1H), 7.47 (s, 1H), 7.02 (d, 1H, J = 8.4 Hz), 6.37–6.26 (m, 3H), 4.32 (s, 2H), 3.66 (s, 3H), 2.02 (s, 9H), 1.70 (s, 6H); MS (EI): 423 (M^+).

Biological evaluation: *Measurement of melanin content:* The cells (2×10^5 cells/mL) were seeded into 24-well plates and derivatives were added in triplicate. The medium was changed daily and after 4 d of culturing, the cells were lysed with 1 mL of 1 N NaOH. Subsequently, 200 μl of each crude cell extract was transferred into 96-well plates. The relative melanin content was measured at 400 nm with a microplate reader (Molecular Devices).

3D QSAR analysis: 3D-QSAR studies were performed using SYBYL-X 2.0 running on a Windows 7 Home Premium K 64 bit OS platform (http://www.tripos.com (St. Louis, MO, 2011)). Each structure of a reasonably low-energy conformation was fully geometry-optimized using a standard Tripos molecular mechanics force field and conjugate gradient with a convergence criterion of 0.05 kcal/mol. Their charges were calculated by the Gasteiger–Huckel method.

References and notes

1. Gupta, A. K.; Gover, M. D.; Nouri, K. N.; Taylor, S. *J. Am. Acad. Dermatol.* **2006**, *55*, 1048.
2. Dalton, S. R.; Gardner, T. L.; Libow, L. F.; Elston, D. M. *J. Am. Acad. Dermatol.* **2005**, *52*, 859.
3. Seo, S.-Y.; Sharma, V. K.; Sharma, N. *J. Agric. Food Chem.* **2003**, *51*, 2837.
4. Kim, Y.-J.; Uyama, H. *Cell. Mol. Life Sci.* **2005**, *62*, 1707.
5. Baek, Y. S.; Ryu, Y. B.; Curtis-Long, M. J.; Ha, T. J.; Rengasamy, R.; Yang, M. S.; Park, K. H. *Bioorg. Med. Chem.* **2009**, *17*, 35.
6. Baek, H. S.; Hong, Y. D.; Lee, C. S.; Rho, H. S.; Shin, S. S.; Park, Y.-H.; Joo, Y. H. *Bioorg. Med. Chem. Lett.* **2012**, *22*, 2110.
7. (a) Halgren, T. A. *J. Comput. Chem.* **1996**, *17*, 520; (b) Kim, D.-C.; Rho, S.-H.; Kim, D.; Kim, S. I.; Jang, C.-S.; Ryu, J. K.; Kim, B. W.; Kweon, C. O.; Kim, H.-K.; Lee, S. J. *Am. J. Biomed. Res.* **2013**, *1*, 43; (c) Martin, T. M.; Harten, P.; Young, D. M.; Muratov, E. N.; Golbraikh, A.; Zhu, H.; Tropsha, A. *J. Chem. Inf. Model.* **2012**, *52*, 2570.
8. (a) Clark, R. D. In *Combinatorial Library Design and Evaluation*; Ghose, A. K., Viswanadhan, V. N., Eds.; Marcel Dekker: New York, 2001; p 337; (b) Clark, R. D. *J. Chem. Inf. Comput. Sci.* **1997**, *37*, 1181; (c) Clark, R. D. *J. Chem. Inf. Comput. Sci.* **1998**, *38*, 1079.
9. Cramer, R. D., III; Patterson, D. E.; Bunce, J. D. *J. Am. Chem. Soc.* **1988**, *110*, 5959.
10. Clark, M.; Cramer, R. D., III *Quant. Struct.-Act. Relat.* **1993**, *12*, 137.
11. Clark, R. D.; Fox, P. C. *J. Comput. Aided Mol. Des.* **2004**, *18*, 563.
12. Clark, R. D.; Sprous, D. G.; Leonard, J. M. In *Rational Approaches to Drug Design*; Höltje, H. D., Sippl, W., Eds.; Prous Science: Barcelona, Spain, 2001; p 475.